Chinese Chemical Letters 34 (2023) 107612

Contents lists available at ScienceDirect

Chinese Chemical Letters

journal homepage: www.elsevier.com/locate/cclet

Organoboron luminophores with extremely strong dual–phase emissions

Qingsong Liu, Man Zhang, Ye Fu, Shen Shen, Liangliang Zhu*

Department of Macromolecular Science, State Key Laboratory of Molecular Engineering of Polymers, Fudan University, Shanghai 200438, China

ARTICLE INFO

Article history:
Received 3 May 2022
Revised 8 June 2022
Accepted 14 June 2022
Available online 18 June 2022

Keywords:
Organoboron
Dual–phase emission
Quantum yield
Rigid-twisted core
Mechanical force

ABSTRACT

Developing efficient dual–phase emission emitters upon organoboron luminophores remains a formidable challenge due to the ubiquitous self–absorption and deleterious π-π interactions from aromatic structure. Here, a new family of benzothiazole–enolate–based organoboron luminophores (**HN1–4**) with effective dual–phase emission was constructed. **HN4** showed almost the highest quantum yield (QY) among this type of compound so far. The three-ring–fused rigid skeleton and moderate intramolecular charge transfer (ICT) effect ensured that **HN4** could give rise to extremely strong emission in any solution (QY up to 99%). X-ray crystallographic analysis showed that the twisted core structure constructed by the boronic coordination of two penta-fluorobenzene of **HN4** was responsible for intense emission in the solid state (QY up to 68%). Besides, **HN4** exhibited a unique response to mechanical force accompanied by a reversible change of the QY. We believe that this strategy provides beneficial inspiration and methodology to design materials with high emissive quantum yield that can be used in a variety of luminescent events.

Design of efficient dual-phase emission (DPE) molecules that can exhibit high emission efficiency both in solution and the solid state is of importance for the development of next-generation advanced optical and biomedical materials [1–5]. Generally, aggregation caused quenching (ACQ) and aggregation-induced emission (AIE) are perhaps the most documented phenomena for luminescent molecules [6–11]. ACQ molecules show strong emission in solution but lose luminescence in the solid state, whereas AIE molecules are just the opposite [11–17]. To date, organic luminophore with high emission efficiency both in solution and the solid state is rare because there exists a large structural gap between AIE and ACQ emitters. Therefore, it is still a great challenge for rationally designing and obtaining DPE luminophores.

Organoboron luminophores have long been the flagship of emissive luminophore complexes due to their outstanding emission properties such as high emission quantum yield in solution and tunable emission from visible to near-infrared light [7,16–23]. However, organoboron luminophores normally show very weak emission in solid state due to ACQ, limiting the practical applications in complex cell microenvironments [3,14]. Thus, researchers have tried different structural methods to improve their emission efficiency both in solution and in solid state. For example, Niu and co-workers reported a classic organoboron luminophore with a good absolute photoluminescence quantum yield (QY) ($\Phi_{F\ in\ solution} = 85\%$, $\Phi_{F\ in\ solid\ state} = 33\%$) by the adjustment of meso–position group [24]. Qi *et al.* applied the AIE strategy to obtain a D–A–D dioxaborine derivative showing moderate emission in solution ($\Phi_{F\ in\ solution} = 20.4\%$) and slightly enhanced one in the solid state ($\Phi_{F\ in\ solid\ state} = 54.5\%$) [25]. These studies have successfully constructed organoboron luminophore showing DPE characteristics, whereas leaving plenty of potential for improvement.

It is known that the emission of traditional organoboron luminophores is quenched in the solid state due to the rigid structure causing deleterious π-π interactions and the self-absorption resulting from very narrow Stokes shifts [26]. Inspired by relevant findings where the gap between rigid structure and self-absorption can be possibly eliminated by structural engineering, herein, we present a rational strategy to create organoboron luminophores for achieving extremely strong DPE. It is expected that based on minimizing the nonradiative transition with a rigid moiety in solution, the twisted core structure can effectively inhibit deleterious π-π interactions in aggregation state. Simultaneously, the emission efficiency of the luminophore can be further enhanced by a moderate intramolecular charge transfer (ICT) effect [27,28]. In this way, **HN1–4** were synthesized *via* a two or three-step procedure shown in Scheme S1 (Supporting information). The three-ring–fused twisted skeleton was constructed *via* the boronic coordination of two penta–fluorobenzene and benzothiazole–enolate

* Corresponding author.
E-mail address: zhuliangliang@fudan.edu.cn (L. Zhu).

https://doi.org/10.1016/j.cclet.2022.06.035
1001-8417/

Table 1
Spectral data of **HN1- HN4** in solution and solid state.

Compound	In solution						In solid state[d]			
	λ_{abs} (nm)	ε (L mol^{-1} cm^{-1})[a]	λ_{em} (nm)	(Φ_F (%)[a, b]	SS (cm^{-1})[c]	τ_f (ns)	λ_{ex} (nm)	λ_{em} (nm)	Φ_F (%)[b]	τ_f (ns)
HN1	371, 382	33,000	446	7	4100	0.33	430	500	10	5.59
HN2	407	42,000	457	82	2680	1.48	462	525	28	10.00
HN3	390, 408	23,000	477	55	3550	2.05	450	500	24	5.89
HN4	429	40,000	509	99	3660	2.40	470	516	68	7.01

[a] Measured at a concentration of 10 μmol/L in toluene at 25 °C.
[b] Absolute photoluminescence quantum yield determined by calibrated integrating sphere systems.
[c] Frequency units between the longest absorption band and emission band in toluene.
[d] Powder examples were used for the absorption and emission measurement.

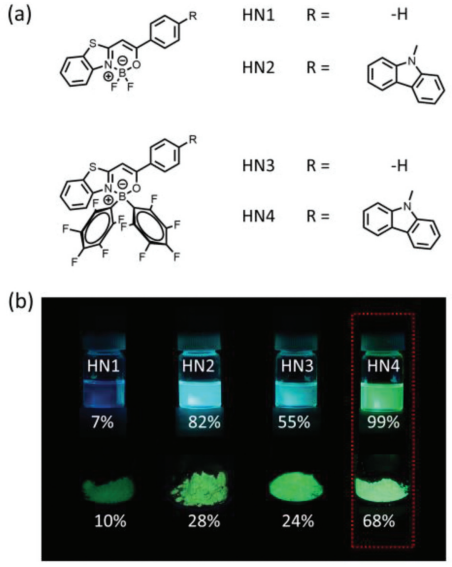

Fig. 1. (a) Chemical structures of compounds **HN1–4**. (b) Luminescent photograph and QY of **HN1–4** in solution and the solid state.

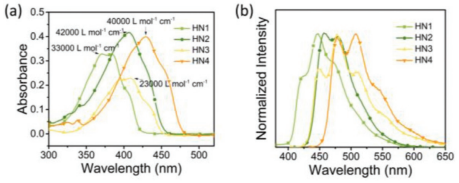

Fig. 2. (a) Absorption and (b) normalized emission spectra of **HN1–4** (10 μmol/L) in toluene at 298 K.

derived ligands. The carbazole group as an electron donor part was harnessed to the boronic core to form D–A type molecules. Here, **HN4** was expected to display unprecedented DPE properties due to an optimization of the twisted core structure and ICT effect. X-ray single-crystal analysis indicated that **HN4** had a twisted boronic core structure, while the density functions theory (DFT) calculation showed that its HOMO was mainly localized on the carbazole group, and its LUMO was mainly localized on the boronic core. This supports the ICT nature of **HN4**.

The photophysical properties of **HN1–4** were measured in solvents with a different polarity and the solid state. The full details can be found in Fig. 2, Table 1, Figs. S1, S2 and Table S1 (Supporting information). In toluene, **HN1** and **HN3** showed an absorption maxima at 382 nm ($\varepsilon = 33{,}000$ L mol^{-1} cm^{-1}) and 408 nm ($\varepsilon = 23{,}000$ L mol^{-1} cm^{-1}), respectively. Compared with **HN1** and **HN3**, **HN2** and **HN4** both showed red shifted absorption bands (~20 nm) with an absorption maxima at 407 nm ($\varepsilon = 42{,}000$ L mol^{-1} cm^{-1}) and 429 nm ($\varepsilon = 40{,}000$ L mol^{-1} cm^{-1}), respectively. Such a red shift of the absorption bands can be explained by ICT enhancement caused by the introduction of carbazole group [26–28]. Besides, compared with **HN1** and **HN2**, **HN3** and **HN4** also exhibited a red shifted (~20 nm) absorption, respectively, suggesting that two penta–fluorobenzene moieties contribute to the ICT effect as well. Besides, due to the weak absorption characteristic of pentafluorophenyl-boron, **HN3** and **HN4** have a lower molar extinction coefficient than **HN1** and **HN2** [27].

From Fig. S1, it is found that the absorption bands of **HN1** and **HN3** were hardly affected by solvent polarity, while **HN2** and **HN4** exhibit somewhat solvatochromic effect due to ICT. The maximum emission wavelength (F_{max}) of **HN1** and **HN3** was at 446 nm and 477 nm, respectively, showing almost no wavelength variation with the change of solvent polarity (Fig. S2). However, their emission intensity was affected by the solvent polarity, indicating that there existed a weak ICT in **HN1** and **HN3**. In contrast, F_{max} and emission intensity of **HN2** and **HN4** were significantly affected by solvent polarity, and two shoulder peaks were observed in low polar solvents due to the mirror image of the absorption spectrum. They showed a dramatically red-shifted emission in high polar solvents such as dimethyl sulfoxide (DMSO), suggesting that the ICT effect played a significant role in the photophysical properties of these molecules [1].

Due to electronic donor effect of carbazole, **HN2** and **HN4** showed strong luminescence in solution (Fig. 3, Figs. S2 and S3 in Supporting information). Notably, as shown in Figs. 3a and b, **HN4** expressed outstanding QY in any organic solvent (*e.g.*, $\Phi_{F\ in\ solution} = 88\%$ in hexane, 99% in toluene, 92% in $CHCl_3$, 33% in DMSO which remained high), suggesting that moderate ICT effect can further enhance the radiative process along with an increased Stokes shift, whereas strong ICT, on the contrary, is a quenching factor due to an enhancement in the rate of nonradiative decay (Table S1) [27,28]. **HN4** showed the highest QY in toluene due to the effect between aromatic molecules and toluene [3]. It is emphasized that the luminescent color of **HN2** changed from blue to yellow with increased solvent polarity (Fig. S3), while **HN4** showed light green in low-polarity solvents and changed to yellow in the high-polarity solvents (Fig. 3a) because of ICT.

In the solid state, **HN1–4** showed a red shifted (about 50 nm) absorption maxima at 430 nm, 462 nm, 450 nm and 470 nm, respectively, compared with those in toluene solution (Table 1). The emission bands of **HN1–4** remained narrow and the F_{max} values (500–525 nm) also underwent a red shift relative to those in toluene solution (Table 1 and Fig. S5 in Supporting information). Such a shift is due to the aggregation–induced CT enhancement [2,7]. While referring to the emission shift, it should be noted that the F_{max} values of **HN1** and **HN2** showed a red shift of more than 50 nm, whereas **HN3** and **HN4** showed a red shift less than 50 nm. These results suggest that twisted structure based on two penta-fluorobenzenes had effectively weakened the deleterious intermolecular π-π interactions in the solid state by increasing the intermolecular spacing, as close molecular stacking could readily

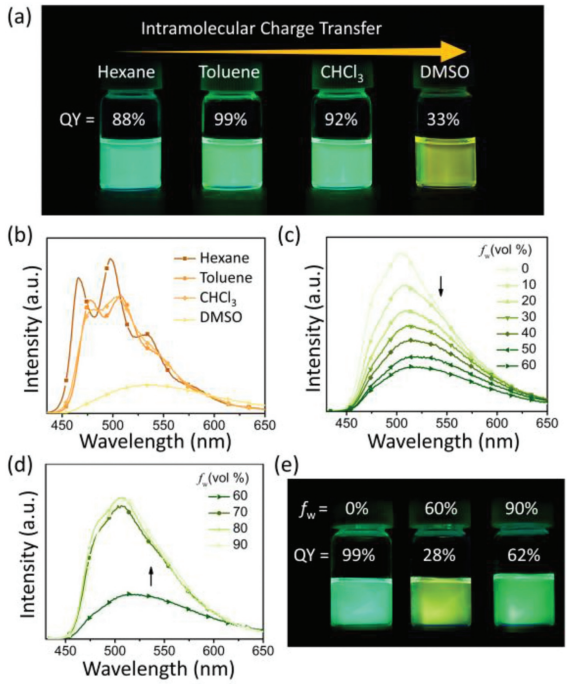

Fig. 3. (a) Photograph under 365 nm UV lamp and (b) emission spectra of **HN4** (10 μmol/L) in hexane, toluene, $CHCl_3$ and DMSO at 298 K, $\lambda_{ex} = 429$ nm. (c, d) Emission spectra ($\lambda_{ex} = 429$ nm) and (e) photograph under 365 nm UV lamp of **HN4** in THF–water mixtures (10 μmol/L) at 298 K with varying volumetric fractions of water (f_w).

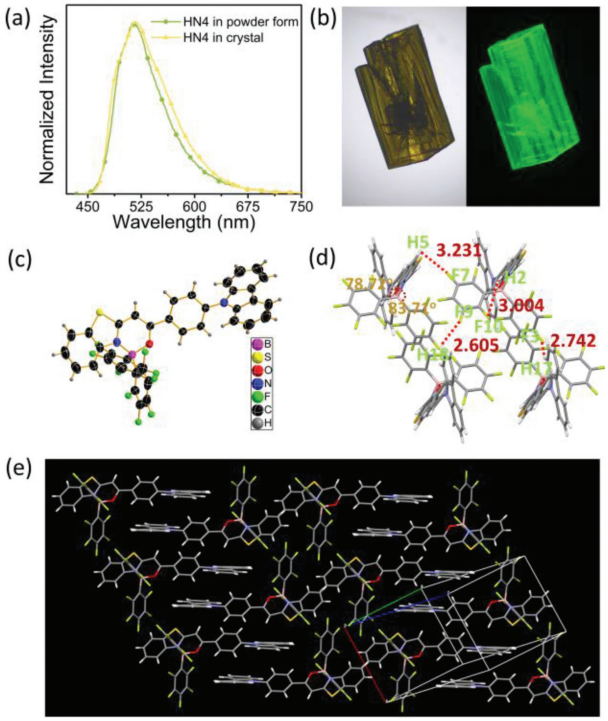

Fig. 4. (a) Emission spectra of **HN4** in the powder and crystal form, $\lambda_{ex} = 470$ nm. (b) Crystal photograph of **HN4** in bright field (left) and under 450 nm laser light (right). (c) Molecular structures of **HN4** (50% probability for thermal ellipsoids). (d) Crystal packing structure of **HN4**. The red dotted lines show intermolecular interactions. (e) Crystal packing structures of **HN4** from a monomolecular layer view.

cause a spectral red-shift [14]. Especially, **HN4** only showed a red shift of 7 nm of its emission in the solid state compared to that in solution, indicating that the π-π interactions for **HN4** are suppressed to a huge degree in the solid state (Table 1).

As expected, **HN1** and **HN3** showed moderate QY in toluene solution ($\Phi_{F\ in\ solution} = 7\% - 55\%$), whereas **HN2** and **HN4** showed outstanding QY ($\Phi_{F\ in\ solution} = 82\% - 99\%$) (Table 1). Importantly, **HN2–4** also showed intense emission in the solid state with a high QY ($\Phi_{F\ in\ solid\ state} = 28\%, 24\%$ and 68%), respectively. Besides, it can be found that only the QY increased significantly upon the introduction of penta–fluorobenzene. The photoluminescence lifetime among **HN1–4** remained at nanosecond scale both in solution and in the solid state. This indicates that the possible isomers in carbazole group have little effect on our study [29]. To the best of our knowledge, **HN4** showed almost the highest dual-phase QY among organoboron luminophores so far. Besides, the photoluminescent lifetime of **HN4** is about 8 times higher than that of **HN1** in solution (Table 1 and Fig. S6 in Supporting information). These results suggest that our strategy of creating high-efficient DPE organoboron luminophore by the unique structural engineering, rigid-twisted core structure with moderate ICT effect, is successful.

To investigate the possible further tunability of QY, the emission spectra of **HN1–4** were investigated in THF/H_2O mixtures with various ratios to compare the photophysical properties of these molecules in different aggregated states (Figs. 3c–e, Fig. S4 in Supporting information). The emission intensity of **HN1** and **HN3** remained almost the same until the water fraction (f_w) reached 80%. Upon addition of 90% water into THF, **HN1** showed large red–shifted emission from 442 to 492 nm and the emission color changed from blue to green, while **HN3** remained the initial emission wavelength and the emission color. On the other hand, **HN2** and **HN4** showed a gradual decrement of the emission intensity with the addition of water into the THF solution till 70% and 60% of f_w, respectively. Further increase of f_w made their emission intensity enhanced again. Especially, **HN4** still showed appreciable luminescence QY (28%), even when the emission intensity turned to be the lowest in f_w of 60%. These results should be largely due to the twisted skeleton constructed *via* the boronic coordination of two penta-fluorobenzene.

In order to better understand the molecular mechanism for these strong emissions, X-ray crystallographic analysis was performed, since there are the same F_{max} values of **HN4** in the solid states as powder form or as crystal form (Fig. 4a). The crystal of **HN4** showed yellow color in bright field and a bright green luminescence under 450 nm laser light in Fig. 4b. The ORTEP (Oak Ridge Thermal Ellipsoid Plot) drawing and molecular packing structure of **HN4** are shown in Fig. 4 and Fig. S10 (Supporting information). The boron atoms adopt a typical tetrahedral geometry to form *N^O*–chelate six-membered ring, which contributes to the construction of the rigid three-ring-fused π-conjugated skeletons. There have been reports showing that intermolecular spacing can be effectively increased after introducing phenyl into boron atom [27,33]. As anticipated, **HN4** adopts rigid–twisted core conformation, making the molecular stacking of **HN4** *J*-aggregation (Fig. 4e). The six-membered ring of the boron core is not on a plane because of the steric hindrance of penta-fluorobenzenes, and the dihedral angle is 24.90°. The dihedral angles of the N-B-O plane and two penta–fluorobenzenes are 78.72° and 83.71°, respectively. The plane of carbazole forms an obvious angle (47.96°) with the N-B-O plane. Intermolecular π-π interactions were not detected in **HN4** upon molecular packing mode. However, multiple short interatomic contacts existed within the crystals: F7···H5–C5 (80.17°, 3.231 Å), F9···H18–C18 (125.34°, 2.605 Å), F10···H2–C2 (154.52°, 3.004 Å), F3···H17–C17 (157.15°, 2.742 Å). Furthermore, C–H···π interactions were detected on 2.869 Å–3.019 Å. These weak intermolecular interactions inhibit the molecular internal rotations

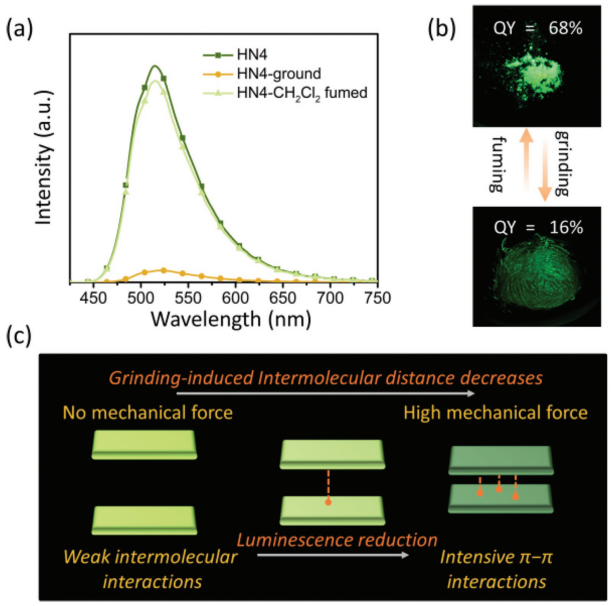

Fig. 5. (a) Emission spectra of **HN4** in the solid state initially, after being ground, and then followed by CH_2Cl_2 fuming, λ_{ex} = 470 nm. (b) Photographs of the powder of **HN4** before and after grinding under UV 365 nm lamp. (c) Proposed mechanism of the molecular switch performance for **HN4**.

and block the non–radiative relaxation, and the twisted skeleton constructed effectively inhibited the π-π interaction, causing **HN4** to show intense emission in the solid state.

To further illustrate the effect of the structure on the electronic structures which are related to the photophysical properties of **HN1**–**4**, DFT calculation was carried out [27]. As shown in Fig. S7 (Supporting information), **HN1** and **HN3** have HOMOs and LUMOs localized over the whole molecules. The calculated first excited state, mainly consisting of HOMO→LUMO transition, has excitation energy of 3.47 eV (358 nm, f = 0.8577) for **HN1** and 3.32 eV (374 nm, f = 0.5863) for **HN3**, respectively. The incorporation of the penta-fluorobenzene group in **HN3** led to an increase of the HOMO and LUMO energy level; however, the HOMO–LUMO gap was decreased. Meanwhile, the incorporation of carbazole group in **HN2** is predicted to greatly increase the HOMO energy level by 0.62 eV, but to have little effect on the LUMO, thus decreasing the HOMO–LUMO gap and resulting in a red-shift of the main absorption band relative to those of **HN1**. The energy levels of HOMOs of **HN2** (3.05 eV, 406 nm, f = 0.5749) and **HN4** (3.00 eV, 414 nm, f = 0.4732) are increased relative to those of **HN1** and **HN3**, due to the introduction of the electron-donating carbazole. The decreased HOMO-LUMO gaps of **HN2** and **HN4** should be responsible for the red-shifted main absorption band relative to those of **HN1** and **HN3**. **HN2** and **HN4** have HOMOs dominated by phenyl-carbazole group, whereas their LUMOs are mostly localized on the benzothiazole and phenyl unit. It is obvious that the lowest-energy excited state for **HN2** and **HN4** corresponds to a charge transfer from the carbazole fragment to the benzothiazole unit. The features of charge transfer make the ground and excited states more energetically distinct, leading to large Stokes shifts and a reduction in self-absorption.

Considering external mechanical force that can often cause structural reorganization in the solid state, resulting in a change of material luminescence signal [30-32], mechanical stimuli responsive properties for **HN4** were also studied (Fig. 5). As expected, the QY of **HN4** was significantly reduced upon grinding with a pestle for 5 min. Its original luminescence of the powder sample was gradually recovered when treated with CH_2Cl_2 vapor for a few minutes. In addition, the grinding led to distinct changes in their powder X-ray diffraction (XRD) patterns (Fig. S8 in Supporting information). All the diffraction peaks of **HN4** were weakened due to the higher amorphization of molecular packing, originating from the decrease of intermolecular distance that resulted in the deleterious π-π interactions and luminescence reduction [32]. However, **HN4** still showed moderate luminescence QY (16%) after grinding, and only the QY difference relative to that of the initial solid state is huge. This perfect reversibility also indicated that such a mechanical grinding is a physical process to change the molecular interaction, rather than any chemical reaction or oxidation effect. This mechanical stimuli-responsive reversible QY alternation endowed the solid state material with superior molecular switch performance.

In summary, we have developed a practical molecular engineering strategy by constructing a rigid-twisted core structure and moderate ICT effect to obtain outstanding DPE organoboron luminophores. The rigid π-conjugated skeletons can enable radiative energy dissipation, allowing luminophore with high emission efficiency in solution, and the twisted core structure of these compounds could enhance the emission efficiency in the solid state by significantly reducing the deleterious intermolecular π-π stacking. Concurrently, the emission efficiency of the luminophore can be further enhanced by a moderate ICT effect. Importantly, **HN4** showed almost the highest dual-phase QY among organoboron luminophores so far. Furthermore, **HN4** is capable of the mechanical force sensibility by the reversible change of QY, which may potentially serve as a superior solid state molecular switch performance. We believe that this could be a valuable strategy to design DPE materials to benefit their practical applications in various luminescent events.

Declaration of competing interest

We declare that we have no known competing financial interests or personal relationships that could have appeared to influence the work reported in this paper.

Acknowledgments

This work was financially supported by the National Natural Science Foundation of China (No. 21975046) and partially from the National Key Research and Development Program of China (No. 2017YFA0207700).

Supplementary materials

Supplementary material associated with this article can be found, in the online version, at doi:10.1016/j.cclet.2022.06.035.

References

[1] J.L. Belmonte-Vázquez, Y.A. Amador-Sánchez, L.A. Rodríguez-Cortés, et al., Chem. Mater. 33 (2021) 7160–7184.
[2] T. Zhang, X. Ma, H. Tian, Chem. Sci. 11 (2020) 482–487.
[3] G. Chen, W. Li, T. Zhou, et al., Adv. Mater. 27 (2015) 4496–4501.
[4] H. Wu, Z. Chen, W. Chi, et al., Angew. Chem. Int. Ed. 58 (2019) 11419–11423.
[5] S. Feng, Z. Qu, Z. Zhou, et al., Chem. Commun. 57 (2021) 11689–11692.
[6] J. Luo, Z. Xie, L. Cheng, et al., Chem. Commun. 18 (2001) 1740.
[7] H. Lu, J. Mack, Y. Yang, et al., Chem. Soc. Rev. 43 (2014) 4778–4823.
[8] Y. Xie, Z. Li, Natl. Sci. Rev. 8 (2021) nwaa199.
[9] X. Jia, C. Shao, X. Bai, et al., Proc. Natl. Acad. Sci. U. S. A. 116 (2019) 4816–4821.
[10] Y. Zhou, J.W. Kim, R. Nandhakumar, et al., Chem. Commun. 46 (2010) 6512–6514.
[11] V. Nguyen, Y. Yim, S. Kim, et al., Angew. Chem. Int. Ed. 59 (2020) 8957–8962.
[12] E. Galbraith, T.D. James, Chem. Soc. Rev. 39 (2010) 3831–3842.
[13] Z. Guo, S. Park, J. Yoon, et al., Chem. Soc. Rev. 43 (2014) 16–29.
[14] K. Li, X. Duan, Z. Jiang, et al., Nat. Commun. 12 (2021) 2376.
[15] H. Dolati, L.C. Haufe, L. Denker, et al., Chem. Eur. J. 26 (2020) 1422–1428.
[16] J. Chen, W. Liu, X. Fang, et al., Chin. Chem. Lett. 33 (2022) 5042–5046.
[17] Y. Zhang, L. She, Z. Xu, et al., Chin. Chem. Lett. 33 (2022) 3277–3280.

[18] M.K. Kuimova, G. Yahioglu, J.A. Levitt, et al., J. Am. Chem. Soc. 130 (2008) 6672–6673.
[19] S. Erbas-Cakmak, S. Kolemen, A.C. Sedgwick, et al., Chem. Soc. Rev. 47 (2018) 2228–2248.
[20] Y. Zhou, Y. Zhuang, X. Li, et al., Chem. Eur. J. 23 (2017) 7642–7647.
[21] H. Li, F. Lv, X. Guo, et al., Chem. Commun. 57 (2021) 1647–1650.
[22] M. Li, S. Long, Y. Kang, et al., J. Am. Chem. Soc. 140 (2018) 15820–15826.
[23] X. Ma, J. Wang, H. Tian, Acc. Chem. Res. 52 (2019) 738–748.
[24] C. Duan, Y. Zhou, G.G. Shan, et al., J. Mater. Chem. C 7 (2019) 3471–3478.
[25] Y. Qi, Y. Wang, G. Ge, et al., J. Mater. Chem. C 5 (2017) 11030–11038.
[26] Q. Liu, X. Wang, H. Yan, et al., J. Mater. Chem. C 3 (2015) 2953–2959.
[27] Y. Wu, H. Lu, S. Wang, et al., J. Mater. Chem. C 3 (2015) 12281–12289.
[28] N. Venkatramaiah, G.D. Kumar, Y. Chandrasekaran, et al., ACS Appl. Mater. Inter. 10 (2018) 3838–3847.
[29] C. Chen, Z. Chi, K.C. Chong, et al., Nat. Mater. 20 (2021) 175–180.
[30] H. Yu, W. Ren, H. Lu, et al., Chem. Commun. 52 (2016) 7387–7389.
[31] Y. Liu, Q. Zeng, B. Zou, et al., Angew. Chem. Int. Ed. 57 (2018) 15670–15674.
[32] X. Wang, Q. Liu, H. Yan, et al., Chem. Commun. 51 (2015) 7497–7500.
[33] Y. Wu, Z. Li, Q. Liu, et al., Org. Biomol. Chem. 13 (2015) 5775–5782.